Korean J. Chem. Eng., 39(9), 2491-2498 (2022)
DOI: 10.1007/s11814-022-1088-1

pISSN: 0256-1115
eISSN: 1975-7220

Enhancing antifouling and separation characteristics of carbon nanofiber embedded poly ether sulfone nanofiltration membrane

Sayed Mohsen Hosseini†, Mansoureh Sadat Banijamali, Samaneh Koudzari Farahani, and Samaneh Bandehali

Department of Chemical Engineering, Faculty of Engineering, Arak University, Arak 38156-8-8349, Iran
(*Received 23 October 2021 • Revised 9 February 2022 • 20 February 2022*)

Abstract−Poly (ether sulfone)-(PES) based mixed-matrix nanofiltration (NF) membranes were fabricated by incorporating carbon nanofibers (CNFs) through solution casting technique. Scanning optical microscopy (SOM), scanning electron microscopy (SEM) and surface roughness analysis were carried out in membrane characterization. Water uptake, contact angle, tensile strength, and porosity measurements, as well as water flux, salt rejection and antifouling experiments were used. SEM images showed more porous structure for the blended membranes compared to virgin membrane. Finger-like pores was also observed for the modified membranes. SOM image showed uniform surface for the prepared membranes relatively. Surface roughness also showed decreasing trend by increase of CNF ratio. Water contact angle was reduced from 67.8° for pristine membrane to 54.6° for the blended membranes. Salt rejection also increased from 66.49% for bare membrane to 86.4% for the blended membrane containing of 0.1 wt% CNFs. The membrane porosity, water content, water flux and tensile strength were enhanced by using CNFs into the membrane body. Blended PES-CNFs membranes showed high fouling resistance compared to the virgin membrane. The flux recovery ratio was measured up to 79.20% for the modified membranes.

Keywords: Nanofiltration Membrane, Carbon Nanofibers, Separation Performance, Antifouling Ability

INTRODUCTION

Membranes have a key role in various industries and different kinds of separation processes [1-3]. Membrane separation technology has gained much attention due to low energy consumption [4,5]. Among the various types, reverse osmosis (RO), microfiltration (MF), ultrafiltration (UF), nanofiltration (NF), membrane distillation (MD) and pervaporation (PV) are frequently used in water filtration [6]. NF membranes have a nominal molecular weight cut-off from 100 to 1,000 Da approximately [7-9]. Several features, including high ability in multivalent ion removal, low operating pressure, reduced cost, and low rejection for monovalent ions make it interesting for water purification. They are also used in variety of fields, including molecular separation of organic solvents [10], pharmaceutical and biotechnology [11], food processing [12], waste treatment [13] as well as desalination [1]. So, development of NF membranes with excellent permeability and selectivity is an important step in their further applications [14]. The wide application of NF membranes in water treatment [15] and desalination [16] causes to produce a large number of polymeric membranes. They have been used to remove different substances such as nitrate and sulfate [19-23], xenobiotics [1], pesticides [17] and heavy metals [18,19] from water.

Different polymers are used in the preparation of NF membranes such as polyetherimide (PEI), polysulfone (PS), cellulose acetate (CA), polyethersulfone (PES), polyimide (PI), polyamide (PA), polyvinylidene fluoride (PVDF), and poly (phenylene ether ether sulfone) (PEES) [20-23]. Various features of PES such as formability, thermal stability, and outstanding mechanical strength lead to its application in many membrane separation processes. However, PES-NF membranes have some disadvantages, including high fouling tendency and low permeability because of low hydrophilicity. There are different approaches to increasing the separation properties of PES membranes, such as surface grafting polymerization, blending with hydrophilic polymers, and use of inorganic fillers in membrane body [24-27]. In recent years, application of nanomaterials in membrane fabrication has increased sharply. Different nanostructures, such as metal/metal-oxide nanoparticles, zeolites, carbon nanomaterials, MOFs and many more, have been used in water filtration [28-34]. Among them, carbon-based nanoparticles, including carbon nanotubes (CNTs), graphene oxides (GO) and carbon nanofibers, have attracted much attention in membrane fabrication and modification due to their extraordinary potential [35]. Shao et al. [36] applied aminated graphene oxide nanoplates in fabrication of thin film NF membranes. The prepared membranes showed high water flux and separation performance related to Na_2SO_4 solution. Wang et al. [37] also studied (attapulgite/graphene oxide) composite membranes for water treatment. Membranes exhibited high water flux besides ~100% dye rejection. In another study functionalized GO nanoplates [38] were utilized in fabrication of PES-NF membrane for $CrSO_4$ removal from water. The salt rejection measured ~95% along with two times flux increasing. In another study Yi et al. [39] prepared pH-responsive (RGO-gCNT) membrane. These membranes showed good separation performance in a wide pH range. Gong et al. [40] also investigated thin film composite NF membrane by including CNT through interfacial polymerization.

†To whom correspondence should be addressed.
E-mail: s-hosseini@araku.ac.ir

The prepared membranes showed long-term stability and excellent separation performance with high rejection of Na_2SO_4 and $MgSO_4$. Guo and colleagues [41] also studied mixed matrix membranes filled with oxidized CNTs and GO. The produced membranes showed good anti-fouling characteristic as well as high pure water flux.

The high aspect ratios, specific surface areas, excellent mechanical properties, interconnected fiber structure, tunable fiber diameter, high chemical stability, partial negative charge and adsorption behavior of carbon nanofibers (CNFs) make it an appropriate candidate in membrane application [42-48]. The earlier studies reported that utilizing CNFs in modification of polymeric membranes led to an improvement in their physico-chemical properties, mechanical stability and separation performance even at low additive concentration. The results also showed a high capacity for natural organic matter (NOM) removal, antifouling property besides high permeate flux for them [49,50]. In the literature, few researches were found on the fabrication of polymeric nanofiltration membranes filled with CNFs. The literature is also silent on characteristic and separation performance of PES-based nanofiltration membranes incorporated by CNFs in water treatment. So, in the current study, PES-based nanofiltration membranes were modified by CNFs. The effect of different CNFs ratios on physico-chemical, separation and antifouling properties of the blended PES-CNFs membranes were studied. Scanning optical microscopy, scanning electron microscopy, 3D surface images, water uptake, contact angle, tensile strength, and porosity measurements as well as water flux, salt rejection and antifouling studies were used in characterization of membranes.

MATERIALS AND METHODS

1. Materials

Polyethersulfone (PES) was supplied by Badische Anilin- and Soda Fabrik (BASF) (Ultrason E6020P, M_W: 58,000). The N, N dimethylacetamide (DMAc, M_w: 87.12 g/mol) was also provided by Merck Inc., Germany. Polyvinylpyrrolidone (PVP, M_W: 25,000) supplied by Merck Inc., Germany also was used as pore former and. Carbon nano fibers (CNFs, Length: 5-50 μm, SSA>18 m^2/g, OD: 200-600 nm, 2.1 g/cm^3) were provided by US Research Nanomaterials, Inc., USA. All other chemicals were supplied from Merck Inc., Germany. Distilled water was also used during the experiment.

2. Preparation of Blended PES-CNFs Membrane

The blended CNFs/PES membranes were prepared by solution casting technique. For the aim, PES and PVP were dissolved initially in DMAc and stirred with mechanical stirring with 200 rpm for 1 h. CNFs with different concentrations were added into the polymeric solution and stirred with mechanical stirring for 4 h. The solutions were then placed in an ultrasonic bath for 1 h and were stored for 24 h to remove the air bubbles at 25 °C. The solutions were cast using an applicator with a thickness of 150 μm on glass plates. Immediately, the plates were dipped in distilled water at 25 °C. To complete the removal of DMAc, the membrane was immersed in distillate water for 24 h. Finally, membranes were placed among two filter paper sheets at 25 °C for 24 h. The composition of polymeric solution is shown in Table 1.

Table 1. The composition of used polymeric solutions in this study

Membranes	PES (wt%)	PVP (wt%)	DMAc (wt%)	CNFs (wt%)
M1	18	1	81.00	0.00
M2	18	1	80.95	0.05
M3	18	1	80.90	0.10
M4	18	1	80.50	0.50
M5	18	1	80.00	1.00

3. Membrane Characterization

3-1. Membrane Morphology

Scanning electron microscopy (SEM, Seron Technology Inc. Korea) and scanning optical microscopy (SOM, Olympus, and model IX 70) were applied to explore the membrane structure. Surface roughness of membranes was investigated by 3D surface image provided using optical microscopy along with SPIP software (version 6.4.1).

3-2. Water Content and Contact Angle

For determining the membrane water content, pieces of membrane were soaked in distilled water for 24 h. Then, they were removed from water and placed between two filter papers to remove extra surface water. They were weighed immediately (OHAUS, Pioneer TM, Readability: 10^{-4} g, OHAUS Corp, USA). Next, the membranes were dried in an oven for 4 h at 60 °C. The amount of water content was determined using the following Eq. (1) [51,52]:

$$\text{Water content}\ (\%) = \frac{W_w - W_d}{W_w} \times 100 \quad (1)$$

where W_w and W_d are the weight of wet and dry membranes.

Surface wettability of prepared membranes was examined by water contact angle measurements using a contact angle measuring instrument. Deionized water as also used as probe liquid. Three different locations were considered to measure the contact angle and to decrease the experimental error.

3-3. Porosity and Pore Size of Membrane

Eq. (2) was applied to determine the average porosity of produced membrane (ε) [2,19]:

$$\varepsilon(\%) = \left(\frac{W_w - W_d}{\rho_f Al}\right) \times 100 \quad (2)$$

where ρ_f is the water density (kg/m^3), A is the membrane effective area (m^2), and l is the thickness of fabricated membranes (m).

Eq. (3) was applied to calculate the mean radius of membrane's pore (r_m) [19,51]:

$$r_m = \sqrt{\frac{(2.9 - 1.75\varepsilon) 8 \eta LQ}{EA\Delta p}} \quad (3)$$

where Q is the water flow rate (m^3/s), η is the water viscosity (8.9×10^{-4} Pa·s) and ΔP is the operating pressure (MPa).

3-4. Flux and Salt Rejection

The dead-end stirred cell (Fig. 1) was employed for study the separation properties of the membranes. The effective area of this cell was 11.94 cm^2. The fabricated membranes were initially pressurized with deionized water for 30 min to achieve a steady pure water flux prior to filtration test. Then, filtration tests were done at

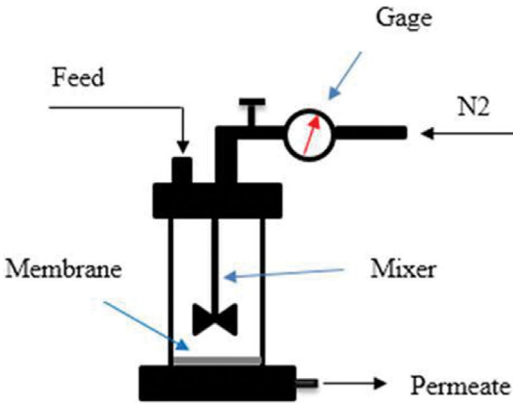

Fig. 1. Schematic diagram of used filtration dead end cell in this study.

a steady pressure (4.5 bar) at ambient temperature. Permeation flux was determined by Eq. (4) as follows [53,54]:

$$J_v = \frac{Q}{A \times t} \tag{4}$$

where J_v (L/m^{2}h) is permeation flux, Q (L) is the amount of permeated water, A (m^2) is effective surface area of membrane and t (h) is the time.

For the determining the salt rejection, a 1,000 ppm Na_2SO_4 aqueous solution was used as feed solution. The following formula was employed for salt rejection calculation:

$$R(\%) = \left(1 - \frac{C_p}{C_f}\right) \times 100 \tag{5}$$

where C_p is concentration of ionic solution of permeate and C_f is

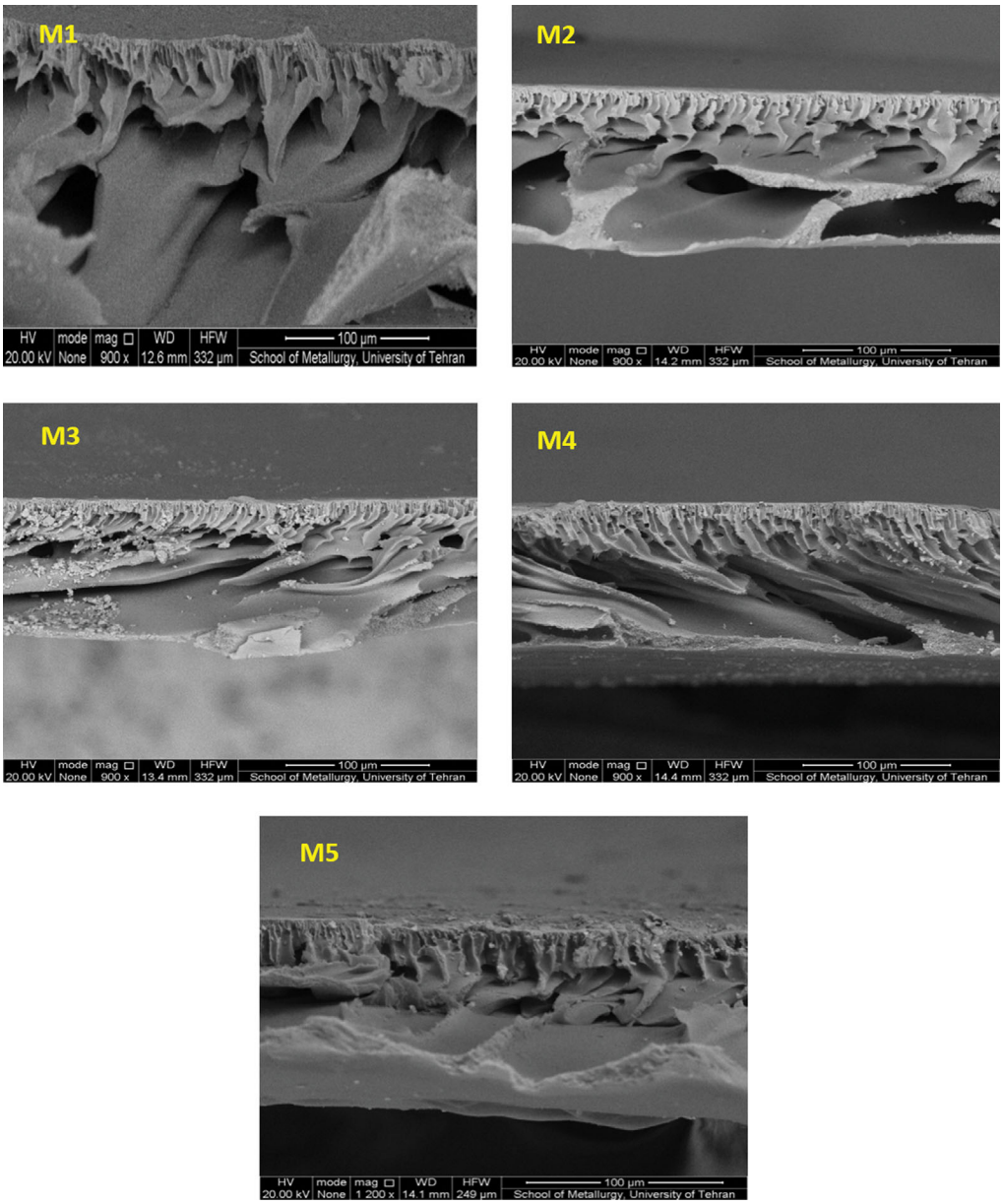

Fig. 2. SEM cross-sectional images of the produced membranes with different dosage of carbon nanofibers.

concentration of ionic solution of feed.

3-5. Mechanical Property of Membrane

The mechanical tensile strength of the fabricated membranes was studied as described elsewhere [55]. For this purpose, membranes were cut into small sizes and the maximum tolerable load of membranes was reported.

3-6. Antifouling Study of Prepared Membranes

First, the pure water flux $J_{w,1}$ (kg/m^2 h) was measured within the cell for 60 minutes. Powder milk solution at a dosage of 8,000 mg/L, as a fouling factor in the stirred cell, was replaced and pressurized for 60 min again. The membranes were then washed and immersed in deionized water for 20 min. Finally, the amount of water flux of washed membranes $J_{w,2}$ (kg/m^{2}h) was measured another time.

The amount of flux recovery ratio (FRR%) was used to study the antifouling ability of membranes as follows [56]:

$$FRR\% = \left(\frac{J_{w,2}}{J_{w,1}}\right) \times 100 \quad (6)$$

Usually, a higher FRR% indicates a better antifouling property for the membranes.

RESULTS AND DISCUSSION

1. Membrane Morphology

Fig. 2 shows the provided cross-sectional SEM images of the fabricated membranes. All membranes showed a porous sub-layer and a dense top layer. As seen, utilizing of CNFs caused the formation of finger-like pores in the membrane sub-layer. As seen, the increasing of CNFs concentration led to an increase of membrane porosity. The porosity of membrane increased from 31.4% for the virgin PES membrane to 67.19% for the blended membrane (M4) with 0.5 wt% CNFs (Table 2). Some decrease of porosity for M5 with 1.0 wt% CNFs is related to possible accumulation of CNFs into the pores at high CNFs concentration. The possible migration of carbon nanofiber into the membrane surface due

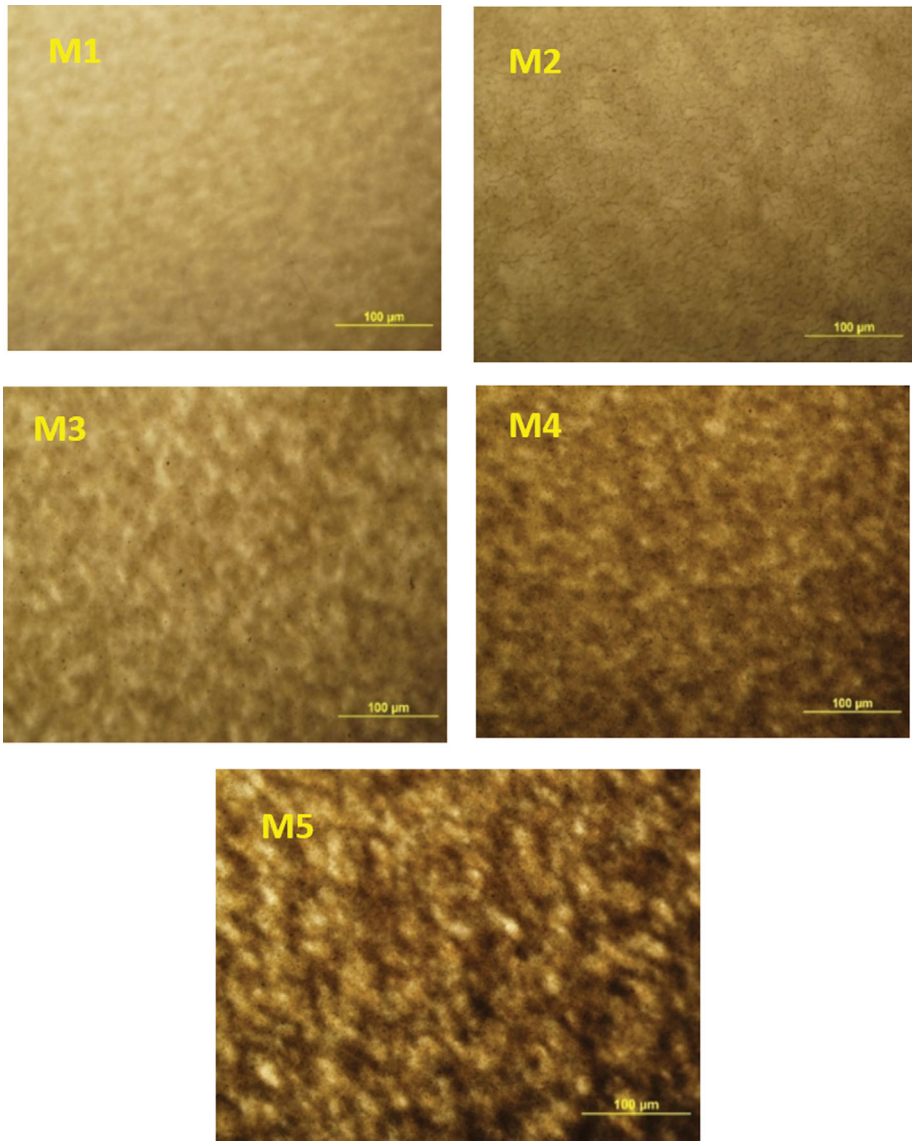

Fig. 3. SOM images of fabricated membranes.

Table 2. The porosity and mean pore size of produced membranes

Membranes	Porosity (%)	Mean pore size (nm)
M1	31.40	1.50
M2	65.70	0.99
M3	65.07	0.86
M4	67.19	0.69
M5	58.42	1.01

to their low density during the phase inversion process provides smoother surface [58] along with more porous structure for the upper layer of membranes. This accelerates the exchange rate between solvent/nonsolvent during the phase inversion process by conducting the water molecules though the upper channels. Moreover, by migration of CNFs into the membrane surface, the thickness of the upper layer enhanced that has an important role in separation performance [2,59-62].

SOM images were used to study the uniformity of the membrane surface. The images (Fig. 3) indicated relatively uniform surface for the prepared membranes. Increase of dark spots for M4 and M5 is related to the possible accumulation of CNFs at high additive concentrations.

3D surface images were utilized to study the membrane surface roughness. As shown in Fig. 4 lowest average roughness (R_a) was obtained for M3. The R_a was reduced from 24.3 nm for M1 to 13.7 nm for M3. This is because of CNFs locating on the membrane surface during the phase inversion process, which creates a smooth surface and fills the valleys. Increase of average roughness for M4 and M5 is also due to the possible accumulation of carbon nanofiber on the membrane surface at high additive concentration.

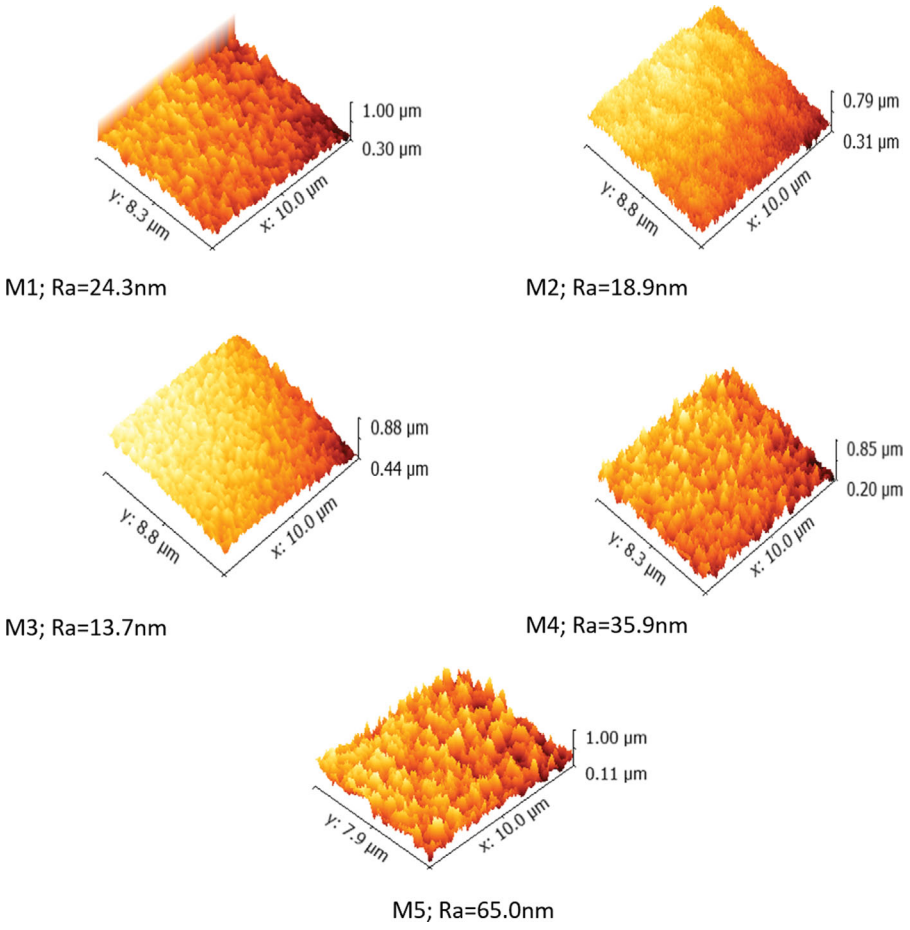

Fig. 4. 3D surface images and surface roughness the for fabricated membranes.

Table 3. Water content for the fabricated membranes

Membranes	Water content (%)	Water contact angle (°)
M1	67.9	67.8
M2	75.06	66.1
M3	73.38	54.6
M4	71.7	56.1
M5	72.7	59.3

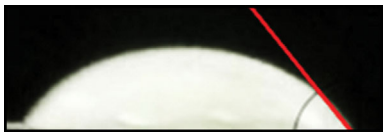

2. The Effect of Carbon Nanofiber Dosage on Water Content and Contact Angle

The effect of different carbon nanofiber dosage on the water content of membranes was investigated. As given in Table 3, all of blended membranes showed a greater amount of water content than the unmodified sample, which can be described by increase of porosity as well as structural heterogeneity that accommodates more water molecules. The water content increased from 67.9% in M1 to 75.06% for M2 due to the increment of membrane porosity. Some reduction of water content at higher CNFs' dosage may be due to pore blocking phenomenon by the CNFs.

According to Table 3, by addition of CNFs into the membrane body the contact angle was reduced. This may be due to smoother surface for the blended membranes that would produce more hydrophilic surface. Some increase in water contact angle at high CNFs ratios is because of CNFs aggregation on the membrane surface [22,63,64].

3. The Mechanical Tensile Strength of Membrane

The results of mechanical strength of the prepared membranes are indicated in Fig. 5. As shown, the mechanical strength of blended membranes, including M2, M3 and M4, is higher than that of the unmodified membrane (M1). It can be concluded that CNFs act as a physical crosslinking factor and thus clinging polymer chains and reduces the slip of polymer chains on each other [65-67]. The mechanical strength of M5 is less than other membranes; this can be due to the aggregation of CNFs in this sample [68]. Besides, reducing of mechanical strength at high CNFs ratio for M5 can be due to increase of channel size for M5 that results in loose membrane structure and reduces the membrane's mechanical strength [60].

4. Effect of CNFs' Ratios on Salt Rejection and Permeability

Permeability and salt rejection are significant factors in determining membrane performance. The effect of CNFs' concentration on flux and rejection is shown in Figs. 6 and 7, respectively. As shown in Fig. 6, the addition of CNFs increased the amount of flux from 3.54 L/m^{2}h for unmodified membrane to 8.37 L/m^{2}h for M5 at 1 wt% of CNFs. The increase of membrane porosity and surface hydrophilicity for modified membranes led to increase of flux.

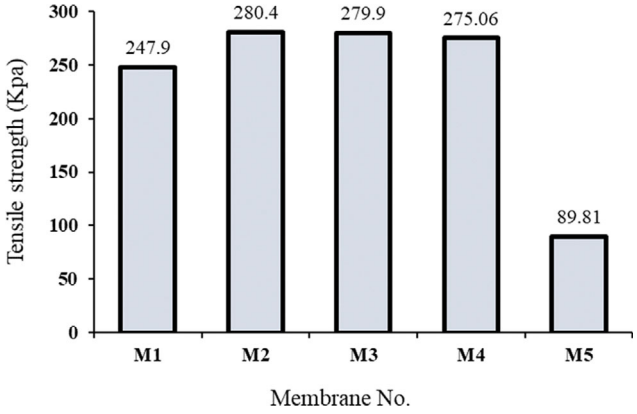

Fig. 5. The mechanical strength behavior of membranes with different CNFs' concentration.

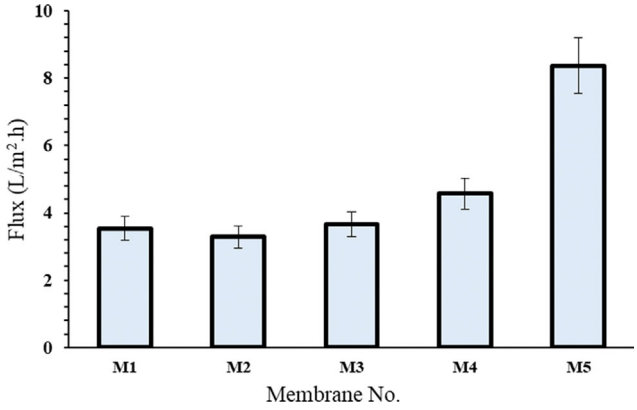

Fig. 6. The effect of carbon nanofiber ratios on the water flux.

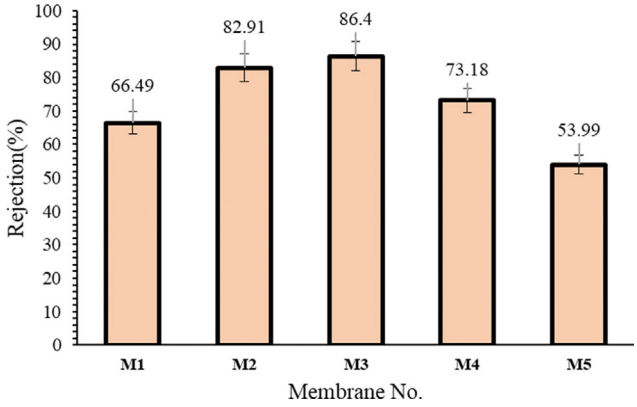

Fig. 7. The effect of carbon nanofiber concentration in member body on salt rejection.

The rejection was increased initially from 66.49% for the bare membrane to 86.4% for M3 with 0.1 wt% CNFs and then decreased to 53.99% for M5 with 1 wt% CNFs. The adsorption property of CNFs would promote deep filtration during the separation process. At high additive concentration, increase of membrane surface roughness caused a decrease of salt rejection due to improving the polarization affects. Furthermore, at high CNFs concentration the possible accumulation of CNFs reduces their active surface area, which

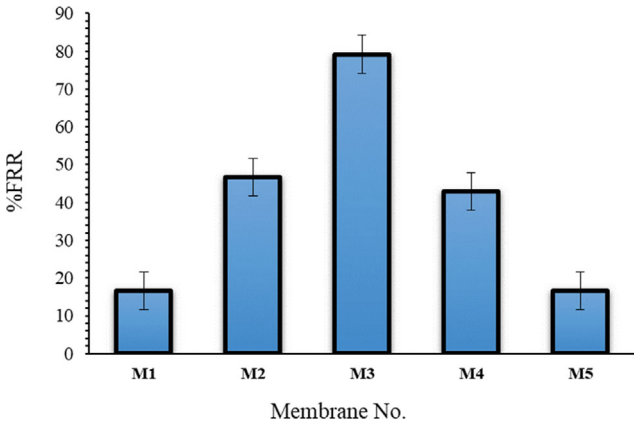

Fig. 8. The amount of FRR% for the fabricated membranes.

Table 4. A typical comparison between prepared membranes in this study with some researches

Membrane	Feed concentration	Pressure	Water Flux ($L/m^2 \cdot h$)	Rejection	Ref
PES-CNFs	1,000 (mg/l)	4.5 bar	3.3-8.4	53.9-86.4	This study
PEI-TiO_2	1,000 (mg/l)	4.5 bar	11.9	69	[3]
PEI-L.POSS.TiO_2	1,000 (mg/l)	4.5 bar	7.9	72	[3]
PI84-GO	0.050 M	15 bar	13.07	>99	[34]

declines the rejection.

5. Antifouling Performance

Separation performance and useful lifetime of the membrane is directly related to the membrane fouling. The membrane flux may reduce with factors like the plugging or blockage of pores inside the membrane as well as the concentration polarization on the membrane surface. The reasons for fouling in membrane are complex. The membrane antifouling feature is usually related to the membrane surface properties [69]. To promote the antifouling property of membranes, many efforts were made to improve membrane surface hydrophilicity [70-72]. To investigate the membrane antifouling properties, the membrane PWF before and after filtration of powder milk solution was compared. The flux recovery ratio (FRR%) was calculated for the aim. The higher amount of FRR% means better membrane antifouling property. The results of FRR% are shown in Fig. 8. The minimum FRR% (16.66%) was measured for the unmodified membrane and the highest amount of FRR% (79.20%) found for M3. The FRR% results were significantly correlated with the membrane hydrophilicity. More hydrophilic surface can adsorb more amounts of water molecules that form a layer on the membrane surface and reduce the adsorption of fouling agents consequently. Besides, as discussed, decrease of membranes surface roughness would reduce the possibility of formation of stagnant layer on the surface that could reduce the fouling deposition on the membrane surface.

A typical comparison between separation performance of fabricated membranes in this study with some reported researches is given in Table 4. As seen, the prepared membranes in the current study are comparable with that of other reported ones.

CONCLUSION

Blended PES-CNFs nanofiltration membranes were fabricated by solution casting technique. The effect of different CNFs concentrations on physico-chemical, separation and antifouling properties of membranes were studied. SEM images exhibited more porous structure for the modified membranes compared to virgin membrane. Finger-like pores were also observed for the blended membranes. SOM image showed uniform surface for the fabricated membranes relatively. Surface roughness was decreased by use of CNF ratios up to 0.1 wt% into membrane matrix and then increased by more additive content. The membrane water uptake, porosity and surface hydrophilicity as well as water flux were increased by embedding CNFs into the membrane matrix. Salt rejection was enhanced from 66.49% for the virgin PES-membrane to 86.4% for (PES-0.1 wt% of CNFs) blended membrane. Furthermore, the use of CNFs in membrane body had a significant effect on their mechanical strength. The blended membranes also showed high antifouling ability compared to the pristine membrane.

ACKNOWLEDGEMENT

Authors gratefully acknowledge Arak University for the financial support during this research. Mansoureh Sadat Banijamali is also thankful Mrs. Faezeh Moradi from Arak University, for the useful help during the experiments.

REFERENCES

1. N. Ghaemi, S. S. Madaeni, A. Alizadeh, P. Daraei, M. M. S. Badieh, M. Falsafi and V. Vatanpour, *Sep. Purif. Technol.*, **96**, 214 (2012).
2. S. Bandehali, F. Parvizian, A. Moghadassi and S. M. Hosseini, *Sep. Purif. Technol.*, **237**, 116361 (2020).
3. S. Bandehali, F. Parvizian, A. Moghadassi, J. N. Shen and S. M. Hosseini, *Korean J. Chem. Eng.*, **37**(9), 1552 (2020).
4. S. Bandehali, A. Kargari, A. Moghadassi, H. Saneepur and D. Ghanbari, *Asia Pacific J. Chem. Eng.*, **9**, 638 (2014).
5. S. Bandehali, A. Moghadassi, F. Parvizian, S. M. Hosseini, T. Matsuura and E. Joudaki, *J. Energy Chem.*, **46**, 30 (2020).
6. A. M. Al Amer, T. Laoui, A. Abbas, N. Al-Aqeeli, F. Patel, M. Khraisheh, M. A. Atieh and N. Hilal, *Mater. Des.*, **89**, 549 (2016).
7. A. Azimi, A. Azari, M. Rezakazemi and M. Ansarpour, *ChemBioEng Rev.*, **4**, 37 (2017).
8. B. Van der Bruggen, *J. Appl. Polym. Sci.*, **114**, 630 (2009).
9. P. Marchetti, M. F. Jimenez Solomon, G. Szekely and A. G. Livingston, *Chem. Rev.*, **114**, 10735 (2014).
10. G. Szekely, M. F. Jimenez-Solomon, P. Marchetti, J. F. Kim and A. G. Livingston, *Green Chem.*, **16**, 4440 (2014).
11. T. O. Mahlangu, T. A. Msagati, E. Hoek, A. Verliefde and B. Mamba, *Phys. Chem. Earth, Parts A/B/C*, **76**, 28 (2014).
12. F. J. Salehi, *Food Bioproducts Process.*, **92**, 161 (2014).
13. O. Agboola, J. Maree, A. Kolesnikov, R. Mbaya and R. Sadiku, *Environ. Chem. Lett.*, **13**, 37 (2015).
14. M. F. Jimenez-Solomon, Q. Song, K. E. Jelfs, M. Munoz-Ibanez and A. G. Livingston, *Nat. Mater.*, **15**, 760 (2016).
15. V. Goncharuk, A. Kavitskaya and M. Skil'skaya, *J. Water Chem. Technol.*, **33**, 37 (2011).
16. S. Ansari, A. Moghadassi and S. Hosseini, *Desalination*, **357**, 189 (2015).
17. B. Tepuš, M. Simonič and I. Petrinić, *J. Hazard. Mater.*, **170**, 1210 (2009).
18. S. Bandehali, F. Parvizian, A. R. Moghadassi and S. M. Hosseini, *J. Polym. Res.*, **26**, 211 (2019).
19. S. Bandehali, A. Moghadassi, F. Parvizian and S. Hosseini, *Korean*

J. Chem. Eng., **36**, 1657 (2019).
20. R. S. Hebbar, A. M. Isloor, K. Ananda and A. Ismail, *J. Mater. Chem. A*, **4**, 764 (2016).
21. M. Ionita, L. E. Crica, S. I. Voicu, A. M. Pandele and H. Iovu, *Polym. Adv. Technologies*, **27**, 350 (2016).
22. A. Moghadassi, E. Bagheripour, F. Parvizian and S. Hosseini, *Int. J. Eng.*, **31**, 1609 (2018).
23. S. Ansari, E. Bagheripour, A. Moghadassi and S. M. Hosseini, *J. Polym. Eng.*, **37**, 61 (2017).
24. S. Hosseini, S. Amini, A. Khodabakhshi, E. Bagheripour and B. Van der Bruggen, *J. Taiwan Inst. Chem. Engineers*, **82**, 169 (2018).
25. T. D. Dipheko, K. P. Matabola, K. Kotlhao, R. M. Moutloali and M. Klink, *Int. J. Polym. Sci.*, **2017**, 3587019 (2017).
26. J. Huang, Z. Shu and Y. Zhang, *Polym. Compos.*, **38**, 908 (2017).
27. Q. Shi, Y. Su, S. Zhu, C. Li, Y. Zhao and Z. Jiang, *J. Membr. Sci.*, **303**, 204 (2007).
28. E. Bagheripour, A. Moghadassi and S. M. Hosseini, *Int. J. Eng.*, **30**, 821 (2017).
29. A. Rahimpour, S. Madaeni, A. Taheri and Y. Mansourpanah, *J. Membr. Sci.*, **313**, 158 (2008).
30. F. Zareei and S. M. Hosseini, *Sep. Purif. Technol.*, **226**, 48 (2019).
31. M. Shaban, H. AbdAllah, L. Said and A. M. Ahmed, *J. Polym. Res.*, **26**, 181 (2019).
32. N. Nasrollahi, S. Aber, V. Vatanpour and N. M. Mahmoodi, *Compos. Part B: Eng.*, **154**, 388 (2018).
33. S. M. Hosseini, M. Afshari, A. R. Fazlali, S. Koudzari Farahani, S. Bandehali, B. Van der Bruggen and E. Bagheripour, *Chem. Eng. Res. Des.*, **147**, 390 (2019).
34. N. K. Zaman, R. Rohani, A. W. Mohammad and A. M. Isloor, *Chem. Eng. Sci.*, **177**, 218 (2018).
35. Y. Manawi, V. Kochkodan, M. A. Hussein, M. A. Khaleel, M. Khraisheh and N. Hilal, *Desalination*, **391**, 69 (2016).
36. W. Shao, C. Liu, H. Ma, Z. Hong, Q. Xie and Y. Lu, *Appl. Surf. Sci.*, **487**, 1209 (2019).
37. C. Y. Wang, W.-J. Zeng, T.-T. Jiang, X. Chen and X.-L. Zhang, *Sep. Purif. Technol.*, **214**, 21 (2019).
38. E. Bagheripour, A. Moghadassi, S. Hosseini, B. Van der Bruggen and F. Parvizian, *J. Ind. Eng. Chem.*, **62**, 311 (2018).
39. G. Yi, X. Fan, X. Quan, H. Zhang, S. Chen and H. Yu, *Sep. Purif. Technol.*, **215**, 422 (2019).
40. G. Gong, P. Wang, Z. Zhou and Y. Hu, *ACS Appl. Mater. Interfaces*, **11**, 7349 (2019).
41. X. Guo, C. Li, C. Li, T. Wei, L. Tong, H. Shao, Q. Zhou, L. Wang and Y. Liao, *Front. Environ. Sci. Eng.*, **13**, 81 (2019).
42. L. Feng, N. Xie and J. Zhong, *Mater. Chem. Front.*, **7**, 3919 (2014).
43. L. Zhang, A. Aboagye, A. Kelkar, C. Lai and H. Fong, *J. Mater. Sci.: Mater. Electron.*, **49**, 463 (2014).
44. M. Ashfaq, N. Verma and S. Khan, *Mater. Sci. Eng.: C*, **59**, 938 (2016).
45. S. Chen, Q. Chen, D. Cai and H. Zhan, *J. Alloys Compd.*, **709**, 304 (2017).
46. K. P. De Jong and J. W. Geus, *Catal. Rev.*, **42**, 481 (2000).
47. M. J. Fernández-Merino, L. Guardia, J. I. Paredes, S. Villar-Rodil, A. Martínez-Alonso and J. M. Tascón, *Rsc Adv.*, **3**, 18323 (2013).
48. C. Kim, Y. I. Jeong, B. T. N. Ngoc, K. S. Yang, M. Kojima, Y. A. Kim, M. Endo and J. W. Lee, *Small*, **3**, 91 (2007).
49. T. Liu, H. Zhou, N. Graham, Y. Lian, W. Yu and K. Sun, *J. Membr. Sci.*, **557**, 87 (2018).
50. X. Cheng, W. Zhou, P. Li, Z. Ren, D. Wu, C. Luo, X. Tang, J. Wang and H. Liang, *Chemosphere*, **234**, 545 (2019).
51. S. M. Hosseini, E. Bagheripour and M. Ansari, *Korean J. Chem. Eng.*, **34**, 1774 (2017).
52. P. Mobarakabad, A. Moghadassi and S. Hosseini, *Desalination*, **365**, 227 (2015).
53. Y. Mansourpanah, S. Madaeni, A. Rahimpour, A. Farhadian and A. Taheri, *J. Membr. Sci.*, **330**, 297 (2009).
54. X. You, T. Ma, Y. Su, H. Wu, M. Wu, H. Cai, G. Sun and Z. Jiang, *J. Membr. Sci.*, **540**, 454 (2017).
55. A. Gholami, A. Moghadassi, S. Hosseini, S. Shabani and F. Gholami, *J. Ind. Eng. Chem.*, **20**, 1517 (2014).
56. V. Vatanpour, S. S. Madaeni, R. Moradian, S. Zinadini and B. J. Astinchap, *Sep. Purif. Technol.*, **90**, 69 (2012).
57. L. Fan, C. Luo, X. Li, F. Lu, H. Qiu and M. Sun, *J. Hazard. Mater.*, **215**, 272 (2012).
58. P. Daraei, S. S. Madaeni, N. Ghaemi, E. Salehi, M. A. Khadivi, R. Moradian and B. Astinchap, *J. Membr. Sci.*, **415**, 250 (2012).
59. E. Bagheripour, A. R. Moghadassi and S. M. Hosseini, *Asia Pacific J. Chem. Eng.*, **10**, 791 (2015).
60. X. Chang, Z. Wang, S. Quan, Y. Xu, Z. Jiang and L. Shao, *Appl. Surf. Sci.*, **316**, 537 (2014).
61. M. R. Mahdavi, M. Delnavaz and V. Vatanpour, *J. Taiwan Inst. Chem. Engineers*, **75**, 189 (2017).
62. S. Zinadini, A. Zinatizadeh, M. Rahimi and V. Vatanpour, *J. Ind. Eng. Chem.*, **46**, 9 (2017).
63. H. Zhang, B. Li, J. Pan, Y. Qi, J. Shen, C. Gao and B. Van der Bruggen, *J. Membr. Sci.*, **539**, 128 (2017).
64. A. Sotto, A. Boromand, S. Balta, J. Kim and B. Van der Bruggen, *J. Mater. Chem.*, **21**, 10311 (2011).
65. S. Zinadini, A. A. Zinatizadeh, M. Rahimi, V. Vatanpour and H. Zangeneh, *J. Membr. Sci.*, **453**, 292 (2014).
66. E. Bagheripour, A. Moghadassi and S. M. Hosseini, *Korean J. Chem. Eng.*, **33**, 1462 (2016).
67. M. Sivakumar, D. R. Mohan and R. Rangarajan, *J. Membr. Sci.*, **268**, 208 (2006).
68. S. Pourjafar, A. Rahimpour and M. Jahanshahi, *J. Ind. Eng. Chem.*, **18**, 1398 (2012).
69. C. H. Koo, A. W. Mohammad and M. Z. M. Talib, *Desalination*, **287**, 167 (2012).
70. R. Kumar, A. M. Isloor, A. Ismail, S. A. Rashid and A. Al Ahmed, *Desalination*, **316**, 76 (2013).
71. D. Rana and T. Matsuura, *Chem. Rev.*, **110**, 2448 (2010).
72. L. Y. Ng, A. W. Mohammad, C. P. Leo and N. Hilal, *Desalination*, **308**, 15 (2013).